1-1-2020

Computer Aided Autism Diagnosis Using Diffusion Tensor Imaging

Yaser A. Elnakieb
University of Louisville

Mohamed T. Ali
University of Louisville

Ahmed Soliman
University of Louisville

Ali H. Mahmoud
University of Louisville

Ahmed M. Shalaby
University of Louisville

See next page for additional authors

IEEE Access
Multidisciplinary | Rapid Review | Open Access Journal

Date of publication xxxx 00, 0000, date of current version xxxx 00, 0000.

Digital Object Identifier 10.1109/ACCESS.2020.DOI

Computer Aided Autism Diagnosis Using Diffusion Tensor Imaging

YASER ELNAKIEB[1], AHMED SOLIMAN[1], ALI MAHMOUD[1], MOHAMED ALI[1], OMAR DEKHIL[1], AHMED SHALABY[1], MOHAMMED GHAZAL[2], ASHRAF KHALIL[2], ANDREW SWITALA[1], ROBERT S. KEYNTON[1], GREGORY N. BARNES[3], AND AYMAN EL-BAZ.[1*]

[1]BioImaging Laboratory, Department of Bioengineering, University of Louisville, Louisville, KY, USA.
[2]Electrical and Computer Engineering Department, Abu Dhabi University, Abu Dhabi, UAE.
[3]Department of Neurology, University of Louisville, Louisville, KY, USA.

Corresponding author: Ayman El-Baz (e-mail: ayman.elbaz@louisville.edu).

ABSTRACT Autism Spectrum Disorder (ASD), commonly known as autism, is a lifelong developmental disorder associated with a broad range of symptoms including difficulties in social interaction, communication skills, and restricted and repetitive behaviors. In autism, numerous studies suggest abnormal development of neural networks that manifest itself as abnormalities of brain shape, functionality, and/or connectivity. The aim of this work is to present our automated computer aided diagnostic (CAD) system for accurate identification of autism based on the connectivity of the white matter (WM) tracts. To achieve this goal, two levels of analysis are provided for local and global scores using diffusion tensor imaging (DTI) data. A local analysis using Johns Hopkins WM areas' atlas is exploited for DTI atlas-based segmentation. Furthermore, WM integrity is examined by extracting the most notable features representing WM connectivity from DTI. Interactions of WM features between different areas in the brain, demonstrating correlations between WM areas were used, and feature selection among those associations were made. Finally, a LOSO classifier is employed to yield a final per-subject decision. The proposed system was tested on a large dataset of 263 subjects from NDAR database with their Autism Diagnostic Observation Schedule (ADOS) scores and diagnosis (141 typically developed: 66 males, and 75 females, and 122 autistics: 66 males, and 56 females), with ages ranging from 96 to 215 months, achieving an overall accuracy of 73%. In addition to this achieved global accuracy, diagnostically-important brain areas were identified, allowing for a better understanding of ASD-related brain abnormalities, which is considered as an essential step towards developing early personalized treatment plans for children with autism.

INDEX TERMS Autism Spectrum disorder, connectivity, diffusion, DTI, dwMRI, gray matter and White matter.

I. INTRODUCTION

Autism spectrum disorder is a neuro-developmental syndrome that affects both communications skills, and behavioral and social interaction [1, 2, 3]. Causes behind ASD are not fully understood, and numerous hypotheses and theories have been proposed for its aetiology . Research suggests that this is a complex or multifactor condition, wherein both genes and environmental influences offer additive effects for symptoms expression. Some investigators hypothesize that ASD symptoms are linked to structural [4] or connectivity [5] anomalies, whereas others suggest a malleable abnormality that ties varying brain functionality to the performance of different tasks [6]. In order to study different types of abnormalities correlated with ASD, several magnetic resonance imaging (MRI) based modalities have been used, such as: (i) structural MRI (sMRI) for studying anatomical features, (ii) functional MRI (fMRI) for studying brain activities, and (iii) diffusion tensor imaging (DTI) for studying brain connectivity. This paper focuses on the latter perspective; using DTI as a way of diagnosing ASD.

DTI has drawn a lot of attention over the last two decades as it allows the analysis of the structural connectivity of the brain white matter (WM) [7]. Although a lot of information could be revealed from the axonal organization, conventional MRI techniques were not capable of capturing this information due to limited resolution and contrast. Fortunately, this has been achievable using DTI, which is characterized by its diffusion anisotropy contrast that reveals information about

axonal orientation. DTI is based on the diffusion of water molecules, which is easier in the direction of the axonal bundles compared to the perpendicular direction, making it feasible to determine axonal direction. In DTI, the diffusion of water molecules is measured along six predetermined directions, from which the diffusion along any arbitrary direction can be calculated. This is mathematically represented by a 3×3 matrix, called the diffusion tensor [8], usually interpreted graphically as an ellipsoid. Several features can be extracted from the diffusion tensor, most importantly, fractional anisotropy (FA), axial and radial diffusivity, and mean diffusivity (MD) [9]. Those measured parameters provide information about WM micro-structure and connectivity [10]. Other features derived from those measurements, such as trace, skewness, rotational invariance, and others, characterize different aspects of diffusivity in WM tracts [11].

Several studies [6, 12, 13, 14, 15, 16, 17, 18, 19, 20] have been carried out using DTI to investigate the presence of abnormalities in the WM in individuals with ASD. [6] used DTI to compare the structure of the white matter of individuals with ASD to that of typically developed (TD) subjects. In their work, they took into consideration IQ, age and gender. They found that the FA had lower values in the case of ASD in some white matter regions of the brain that are known to be associated with social cognition e.g., temporoparietal junction, superior temporal sulcus, ventromedial prefrontal cortex, fusiform gyrus, and anterior cingulate; however, their study did not report any alterations that might occur to the MD values. In addition to FA values, MD values were also obtained by [12] for the corpus callosum. Their work showed a reduction in the FA values and an increase in the MD values of the total corpus callosum for individuals with ASD as compared to TD subjects. Higher MD and radial diffusivity with reduced FA in autistic subjects was reported by [13]. Another study [14] examining the frontal lobe white matter reported FA values and a higher diffusion coefficient in ASD.

The integrity of WM was examined using DTI by [15] for ASD and TD subjects with and without age and IQ correction. The individuals with ASD were found to have a higher MD over the WM of the cerebellum and cerebrum, regardless whether the correction was performed or not. They also noted decreased FA values for the left and right superior and inferior longitudinal fasciculus, and in the left corona radiata in cases of ASD when age and IQ were taken into consideration; however, this decrease almost disappeared after performing age and IQ correction. Their analysis inferred that the kurtosis of the distribution of FA values of WM is higher in cases of ASD. [16] presented a comprehensive review on 48 studies that were carried out from 2004 to 2012 for the purpose of studying the WM integrity of ASD using DTI. The review showed an agreement between these different studies in that individuals with ASD have lower WM integrity over many regions of interest as compared to TD individuals, reflected as lower values of FA and higher values for MD. The results were highly consistent in regards to some regions of interest, e.g., cingulum, corpus callosum. [19] reviewed some of the current structural and functional connectivity ASD data to examine the 'disrupted connectivity' theory. They identified many confounds in the literature that could have affected the conclusions and highlighted the conflicting results. In [20], correlations between autism-spectrum quotient (AQ) and DTI parameters (FA, MD, AD, RD) were examined in white matter tracts that were altered in previous studies for obsessive-compulsive disorder (OCD) patients with ASD traits. Their results suggested that variations in WM features may be explained partially by autistic traits in OCD patients.

In one study of 75 subjects, [21] showed a diagnostic predictive capability, with 80% accuracy, based on FA and MD. Another study that aimed to provide classification of autism, performed on 73 subjects used the shape of white matter tracts to achieve an accuracy up to 75% [22]. In [18], WM connectivity was analyzed and its integrity was used in the diagnosis of autism in 38 balanced-groups of infants.

As concluded from similar investigations, neither the under-connectivity nor the over-connectivity of the brain hypothesis can successfully describe the deviations of the ASD population alone [23]. Despite the numerous efforts to detect autism-related variations using imaging, there is no robust, effective CAD system that is able to both diagnose autistics and place them within a severity spectrum. This is what originated the idea of using DTI in order to develop an extensive automated diagnosis system that can resolve autism endophenotypes and help the clinician deliver personalized treatment plans to individuals with autism.

II. METHODOLOGY

The primary objective of this work is to extract informative local white matter features for each brain area that can be used to discriminate an autism diagnosis. Fusing the results of those local associations would help obtain an accurate global diagnostic decision per subject. The framework mainly consists of three stages: first, a preprocessing step is carried out to reduce imaging artifacts and eliminate non-brain tissues. The second stage is feature calculation, extraction, and selection, including the use of an atlas-based segmentation technique to allocate features for each area. The third stage is a classification step that is used for obtaining the final diagnosis, as well identifying specific brain areas that offer best help to differentiate ASD from neurotypical. Details of the proposed framework as well as experimental results are discussed in the next sections.

A. WHITE MATTER CONNECTIVITY ANALYSIS:

For each subject, white matter was studied using diffusion tensor imaging (DTI) information. In DTI, a 3x3 diffusion tensor describes the behavior of each voxel. To find the principal diffusion directions, the 3 eigenvalues λ_1, λ_2, and λ_3 and their corresponding eigenvectors v_1, v_2 and v_3 are calculated, where the eigenvector corresponding to the largest eigenvalue is the principle diffusion direction (i.e, diffusion across the fiber) while the other two eigenvectors correspond

This article has been accepted for publication in a future issue of this journal, but has not been fully edited. Content may change prior to final publication. Citation information: DOI 10.1109/ACCESS.2020.3032066, IEEE Access

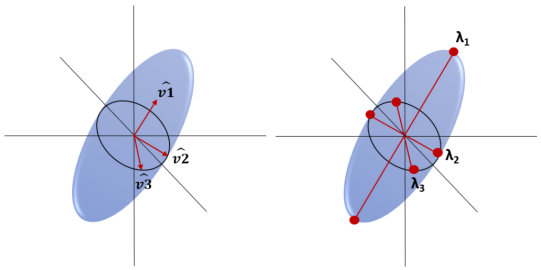

(a) Tensor eigenvectors (b) Tensor eigenvalues

FIGURE 1: Graphical representation of diffusion tensor using the ellipsoid model using three eigenvectors that define the orientation of the ellipsoid in 3D, and three eigenvalues that define the principal axes values of the ellipsoid.

to the radial diffusion directions (i.e,diffusion perpendicular to the fiber) as illustrated in FIGURE 1 [24].

A special case is an isotropic medium, where the diffusion ellipsoid takes the shape of a sphere where $\lambda_1 = \lambda_2 = \lambda_3$. In the case of an anisotropic medium, the diffusion is represented as an ellipsoid as shown pointing in the v_1 direction of λ_1. There are six output features obtained from DTI that are the most commonly used anisotropy measurements describing white matter connectivity:

1) Fractional Anisotropy (FA): The most widely used measurement of anisotropy, a scalar value between 0 and 1 that determines the diffusion integrity. As FA approaches 0, the diffusion is considered to be isotropic while higher values mean that the diffusion tends to be in a uniform direction (i.e,the principal eigenvector direction) [24, 25].
2) Mean diffusivity (MD): Average diffusion measurement that gives an overall assessment of the diffusion in a voxel, $\mathrm{MD} = \frac{1}{3}(\lambda_1 + \lambda_2 + \lambda_3)$.
3) Axial diffusivity (AD): Measures the diffusion along the principal axis. $\mathrm{AD} = \lambda_1$.
4) , 5) Radial diffusivity in the two perpendicular vectors to the principle diffusion vector: $\lambda_2 and \lambda_3$.
6) Skewness: a 3^{rd} order measurement, characterizing the shape of the diffusion tensor, which is not captured by FA or other lower order measurements [11]. $Skewness = \frac{(\lambda_1 - MD)^3 + (\lambda_2 - MD)^3 + (\lambda_3 - MD)^3}{3}$.

In the present study, FSL toolbox https://fsl.fmrib.ox.ac.uk was used for DTI computation. The eddy current correction [26] and brain extraction using BET algorithm [27, 28] were applied prior to calculating the diffusion tensor. FIGURE 2 shows an example of the tensor visualization.

The calculated features are then aggregated over the 48 local regions defined by Johns Hopkins WM atlas parcellation [29] using DTI-TK software. The atlas-based segmentation task is elaborated in the next subsection. Finally, the rest of the proposed algorithm is implemented in Matlab.

1) Brain parcellation into local brain areas:

After calculating the above metrics at each vertex, it is important to allocate those metric values into local brain regions. An atlas-based segmentation approach is adopted, where we treat the area's segmentation problem as a registration task. In this step, Johns Hopkins WM atlas [29] along with its labeled areas are used. John Hopkins is an ICBM coordinate-based WM atlas which defines 48 brain areas that were hand segmented from 81 different subjects. A registration from the MNI atlas space to each subject's space using DTI-TK software [30] is performed, as it supports interoperability with FSL. After atlas-subject registration, an affine transformation is applied to JHU atlas labels, providing WM areas masks for each subject. Thus, we can get local features for each WM area that are used at the local classification level.FIGURE 3 shows the entire diagnosis pipeline. The main advantage of this technique is that it is scalable, automated, and has high accuracy.

2) Feature selection:

The above mentioned procedures provide 6 features (FA, MD, λ_1, λ_2, λ_3, and Skewness) for each voxel, per each subjects. All of those are raw values per voxel, some vectors are tens of thousand in length per area. To provide a compact representation, we calculate a short summary statistics vectors (mean [μ], standard deviation [σ], and skewness [$E(x-\mu)^3/\sigma^3$]) for each area. Then, we concatenate those summary statistics resulting in a feature vector of length 18 per each area (6 feature types $\times$ 3 summary statistic vector length). Instead of using those direct features, we derive new ones capturing the implicit relationships between different brain areas' values, calculated as the correlation between the feature vectors of each two areas. We reduce this huge feature space(48×48 per subject), relative to the sample size (263 subjects), by extracting only the important discriminatory features, to build our diagnosis algorithm. For this purpose, we used a simple filtering method known as the signal to noise ratio (s2n) filter [31]. In this method, we rank each feature based on a score representing the ratio between the absolute difference of the means of the two classes and their variance, given by

$$s2n(X_i, Y) = \frac{abs(\mu(y_+) - \mu(y_-))}{var(y_+) + var(y_-)} \quad (1)$$

where X_i is the feature vector, and Y is class label, $\mu(y_+)$ is the mean value for class y_+ vectors, and $var(y_+)$ is the variance for this class. FIGURE 4 illustrates the adopted feature selection technique. Then, we use only the highest-ranking features in next steps.

B. ASD DIAGNOSIS

Using the local features extracted from DTI, each of the extracted feature for each of the white matter areas were used separately to distinguish between ASDs and TD subjects on the global level. The contribution of each added feature on the diagnostic accuracy is shown, highlighting those that were most related to autism. A number of classifiers from diverse classifier algorithms were tested, including Support Vector

This article has been accepted for publication in a future issue of this journal, but has not been fully edited. Content may change prior to final publication. Citation information: DOI 10.1109/ACCESS.2020.3032066, IEEE Access

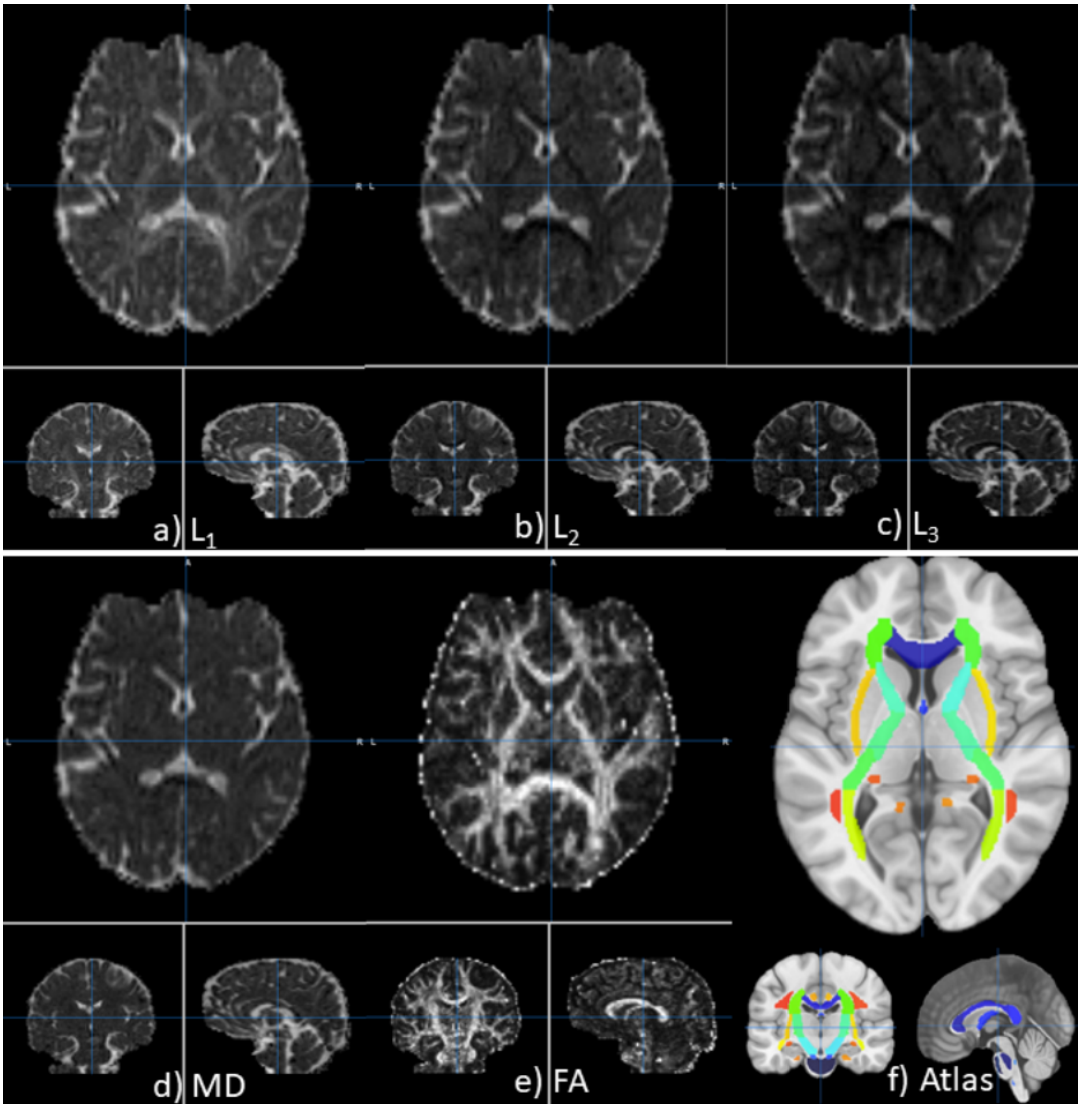

FIGURE 2: Example of extracted features from one subject DTI brain, (a) Axial diffusivity λ_1 , (b) Radial diffusion λ_2, (c) Radial diffusion λ_3, (d) Mean Diffusivity MD, (e) Fractional Anisotropy FA, (f) Labeled WM areas of John Hopkins Atlas, each color identifies here different WM area.

Machine, k-Nearest Neighbor (KNN), decision trees, neural networks (NN), and deep NN with auto-encoders and experiments show better performance in terms of cross-validated accuracy and time for Support Vector Machine (SVM). Linear SVM-classifiers were used on each classification level, that takes correlation features as inputs and outputs a probability that a subject is autistic from the given areas for which information is provided. Normally, not all areas will give significant discrimination between autistic and TD subjects, so first n features, are used in classification, where n is determined empirically. FIGURE 3 shows the pipeline of the entire diagnostic framework.

III. EXPERIMENTAL RESULTS

Data for this experiment were obtained from the National Database for Autism Research (NDAR) [32]. Anonymized MRI scans were obtained for 263 subjects (131 females and 132 males, 122 autistic and 141 typically developed). The subjects' ages were between 96 to 215 months, and they had IQs ranging between 84 and 118.

To ensure system robustness, we used leave-one-subject-out (LOSO) cross-validation at all runs. For each WM area, overall accuracy, sensitivity, and specificity were calculated.

To obtain the subject's global diagnosis decision, two steps are used. First, features are ranked based on the s2n score, then iteratively first n is fed to next step, with n starting from 1 to 250. Selected features are concatenated, and SVM classifiers are used to obtain probabilities of being autistic given this new feature vector, providing a single global decision per subject, which achieved a diagnostic accuracy of 73%, sensitivity of 70%, and specificity of 76%. This performance was achieved using n = 79 correlations. The most significant of these region

This article has been accepted for publication in a future issue of this journal, but has not been fully edited. Content may change prior to final publication. Citation information: DOI 10.1109/ACCESS.2020.3032066, IEEE Access

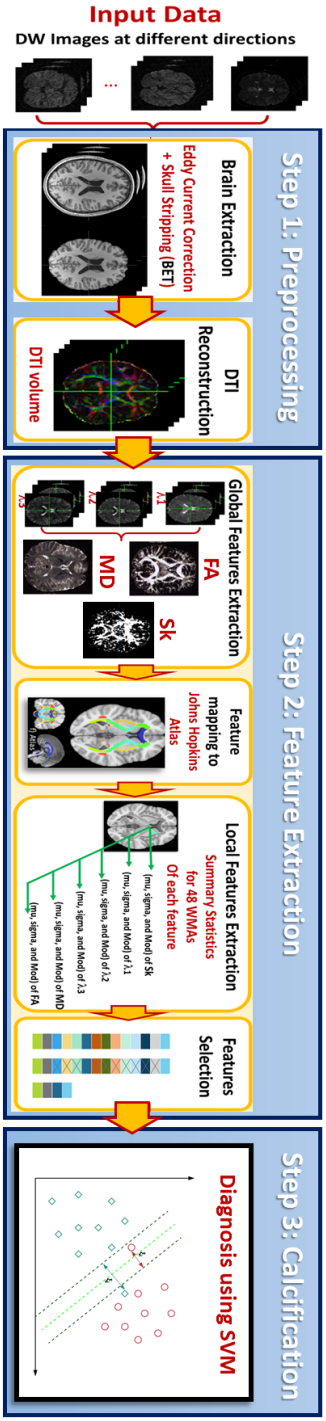

FIGURE 3: DTI experiment pipeline, where the brain is extracted, preprocessed, features calculated, atlas based segmentation performed, and selected features are incorporated for final classifiers.

Algorithm 1 DTI-based ASD diagnosis system

$\forall$ **dwMRI subject's data** :
1. run preprocessing modules:
i) Eddy Current Correction
ii) Apply brain mask generated by Brain Extraction Tool
2. Feature Calculations:
i) Use FSL to calculate DTI Tensor, scale units, calculate λ_1,λ_2,λ_3,FA,MD, sk volumes
ii) Register DTI MNI space IIT Human Brain Atlas to each subject using DTI-TK
iii) Apply resulted transformation on the JHU atlas labels
iv) Use registered labels to extract feature per each WM area
v) Calculate summary statistics (μ, σ, $Skwns$) for each area for each feature, rank feature values across the different 48 brain areas, get feature vector.
vi) Calculate correlations between feature vectors of each two areas
vii) Use s2n filter to rank correlation-features
3. Classification:
i) iterate on n from 1 to 250.
ii) Feed first n ranked ordered feature for all subjects to an SVM classifier
iii) Give a final diagnosis for each subject, whether TD or ASD
End.

TABLE 1: Top ten pairs of white matter areas whose feature-vector correlations provides separability with highest rank according to s2n filter. Regions represented in both hemispheres are annotated with L (left) or R (right) if only one hemisphere is involved, or with B (bilateral) otherwise.

Rank	Area 1	Area 2
1	Superior longitudinal fasciculus R	Anterior corona radiata R
2	Body of corpus callosum	Genu of corpus callosum
3	Superior longitudinal fasciculus R	Sagittal stratum
4	Tapetum L	Middle cerebellar peduncle
5	Splenium of corpus callosum	Middle cerebellar peduncle
6	External capsule L	Middle cerebellar peduncle
7	Cingulum L	Corticospinal tract R
8	Stria terminalis R	Superior corona radiata L
9–10	Superior longitudinal fasciculus L	Posterior corona radiata B

pairs are listed in TABLE1.

IV. DISCUSSION

The most important regional correlations for distinguishing ASD from control 1 are a diverse group, but they fall into five categories. First is the middle cerebellar peduncle (mcp) as it correlates with the splenium of the corpus callosum, the left external capsule (ec), and the left tapetum. The uncinate fasciculus is a fiber pathway through the ec, which links the ventral frontal cortex, in particular Brodmann areas 11 and 47, with the temporal pole [33]. Commissural fibers of the

This article has been accepted for publication in a future issue of this journal, but has not been fully edited. Content may change prior to final publication. Citation information: DOI 10.1109/ACCESS.2020.3032066, IEEE Access

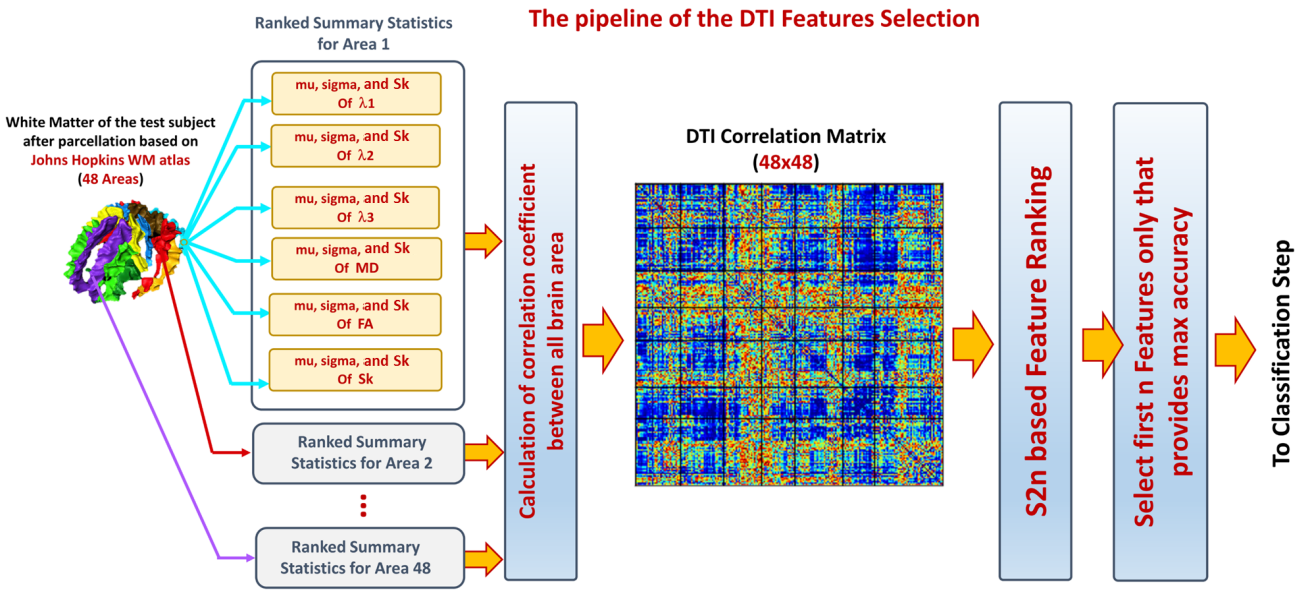

FIGURE 4: DTI feature extraction procedure

left temporal pole, and of the temporal lobe in general, pass through the left tapetum on their way to or from the splenium. The mcp on the other hand carries signals from the cerebral cortex and subcortical regions, via the pontine nuclei, into the cerebellar cortex.

Next are correlations between the superior longitudinal fasciculus (SLF) on the right hemisphere with ipsilateral sagittal striatum (SS) and anterior corona radiata (CR), and between SLF in the left hemisphere with bilateral posterior CR. The SLF is a bidirectional pathway along the anterior-posterior direction through which different lobes communicate with each other [34]. Thalamocortical fibers pass through the SS and CR, where they intermingle with callosal axons [35]. In this category as well as the first, we see in ASD a difference in the microstructure of cortico-cortical pathways relative to pathways linking the cerebral cortex with outside regions.

Output from the left motor cortex passes through the corticospinal tract on the opposite side. Communication between left motor and premotor areas meanwhile makes use of pathways through the left cingulum. The middle segment of the cingulum would be involved in particular; however, the atlas used in this study does not parcellate the cingulum further, so we were only able to identify altered correlation between left cingulum as a whole and right corticospinal tract. Still, this once again suggests changes in a cortical area's connectivity with elsewhere in the cortex vis-à-vis regions outside the cortex.

The superior CR contains sensorimotor fibers of the posterior frontal/anterior parietal cortex. The microstructure of this region by itself has been found to differ between ASD and typically developing children [36]. The stria terminalis contains efferent fibers from the amygdala, which terminate in several nuclei of the hypothalamus and regulate the stress response. We might hypothesize that the increased stress response seen in ASD [37] is normal hypothalamic activation triggered by abnormal sensory processing. While the differences in the superior CR found by Pryweller and colleagues [36] were more pronounced in the left hemisphere, statistical testing did not find this significant. Nor was there any significant distinction between superior CR and other sensory processing pathways they investigated; all showed increased apparent diffusivity in ASD. It is not clear why in our study left superior CR, relative to stria terminalis, particularly stood out.

Differences in the microstructure of genu and body of the corpus callosum relative to each other are harder to interpret, given that they are complementary parts of the same structure, containing commissural fibers from distinct regions of the cortex. It may be of significance that the sections of the corpus callosum develop at different gestational ages. The axons forming the genu grow first, starting in the twelfth or thirteenth week of gestation, followed by the body and splenium in anterior-posterior order, and finally the rostrum [38]. Could this be a clue to pinpointing the developmental stage at which the propensity for developing ASD originates?

There remain many challenges and potential enhancements to be investigated in future work. Whilst the system is well tested and its robustness is assured on only parts of our dataset, different datasets are needed to assure the generalizability of the results. Also, more medical interpretation and statistical analysis are needed to map the impacted regions to the corresponding expected behaviors. The differences in regional correlations we have found so far will be useful for constructing testable hypotheses in that regard. Though many registration tools were tested on the dataset bulk, a tailored manual enhancement for area parcellation of each subject can lead to better feature details and hence improved performance.

Although the system is well tested and its robustness is assured on current dataset, more datasets is needed to

check the extendibility and generalization of the results. Verifying the proposed framework on different dataset would validate the result and enhance findings. The next steps for our implemented CAD is to include different image modalities, such as structural or functional MRI. In this way, the CAD system will be able to study shape, connectivity and even functionality, getting most informative abnormality measures, which might enhance its accuracy, provide better understanding and personalization, towards an integrated full system for autism prediction and diagnosis.

A. CONCLUSION

In summary, the proposed diagnosis framework achieved various goals. First, beside accomplishing a high diagnostic decision, it allows for a better understanding of the areas in the white matter impacted by ASD instead of just deciding whether a subject is autistic. This should in turn lead to a better understanding of an autistic individuals' behavior and predictability of disorder development for those at risk. The reported accuracy is in the high-range of those reported in the literature using DTI, with a larger sample size of 263 subjects. In addition, our system offered scalability, where additional data sources or imaging modalities could be integrated to the model, and its contribution to the decision could be considered separately or jointly.

REFERENCES

[1] American Psychiatric Association, Diagnostic and statistical manual of mental disorders, fifth edition (DSM-5). Arlington: American Psychiatric Association, 2013.

[2] M. F. Casanova, A. El-Baz, and J. S. Suri, Autism Imaging and Devices. CRC Press, 2017.

[3] M. Ismail, R. Keynton, M. Mostapha, A. ElTanboly, M. Casanova, G. Gimel'farb, and A. El-Baz, "Studying autism spectrum disorder with structural and diffusion magnetic resonance imaging: a survey," Frontiers in human neuroscience, vol. 10, 2016.

[4] S. Brieber, S. Neufang, N. Bruning, I. Kamp-Becker, H. Remschmidt, B. Herpertz-Dahlmann, G. R. Fink, and K. Konrad, "Structural brain abnormalities in adolescents with autism spectrum disorder and patients with attention deficit/hyperactivity disorder," Journal of Child Psychology and Psychiatry, vol. 48, no. 12, pp. 1251–1258, 2007.

[5] M. Noriuchi et al., "Altered white matter fractional anisotropy and social impairment in children with autism spectrum disorder," Brain research, vol. 1362, pp. 141–149, 2010.

[6] N. Barnea-Goraly et al., "White matter structure in autism: preliminary evidence from diffusion tensor imaging," Biological Psychiatry, vol. 55, no. 3, pp. 323–326, 2004.

[7] S. Mori and J. Zhang, "Principles of diffusion tensor imaging and its applications to basic neuroscience research," Neuron, vol. 51, no. 5, pp. 527–539, 2006.

[8] P. Hagmann, L. Jonasson, P. Maeder, J.-P. Thiran, V. J. Wedeen, and R. Meuli, "Understanding diffusion mr imaging techniques: from scalar diffusion-weighted imaging to diffusion tensor imaging and beyond," Radiographics, vol. 26, no. suppl_1, pp. S205–S223, 2006.

[9] L. J. O'Donnell and C.-F. Westin, "An introduction to diffusion tensor image analysis," Neurosurgery Clinics, vol. 22, no. 2, pp. 185–196, 2011.

[10] D. K. Shukla et al., "Tract-specific analyses of diffusion tensor imaging show widespread white matter compromise in autism spectrum disorder," Journal of Child Psychology and Psychiatry, vol. 52, no. 3, pp. 286–295, 2011.

[11] P. J. Basser, "New histological and physiological stains derived from diffusion-tensor mr images," Annals of the New York Academy of Sciences, vol. 820, no. 1, pp. 123–138, 1997.

[12] A. L. Alexander, J. E. Lee, M. Lazar, R. Boudos, M. B. DuBray, T. R. Oakes, J. N. Miller, J. Lu, E.-K. Jeong, W. M. McMahon et al., "Diffusion tensor imaging of the corpus callosum in autism," Neuroimage, vol. 34, no. 1, pp. 61–73, 2007.

[13] J. E. Lee et al., "Diffusion tensor imaging of white matter in the superior temporal gyrus and temporal stem in autism," Neuroscience Letters, vol. 424, no. 2, pp. 127–132, 2007.

[14] S. K. Sundaram et al., "Diffusion tensor imaging of frontal lobe in autism spectrum disorder," Cerebral Cortex, vol. 18, no. 11, pp. 2659–2665, 2008.

[15] W. B. Groen, J. K. Buitelaar, R. J. Van Der Gaag, and M. P. Zwiers, "Pervasive microstructural abnormalities in autism: a dti study," Journal of psychiatry & neuroscience: JPN, vol. 36, no. 1, p. 32, 2011.

[16] B. G. Travers, N. Adluru, C. Ennis, D. P. Tromp, D. Destiche, S. Doran, E. D. Bigler, N. Lange, J. E. Lainhart, and A. L. Alexander, "Diffusion tensor imaging in autism spectrum disorder: a review," Autism Research, vol. 5, no. 5, pp. 289–313, 2012.

[17] Y. Aoki, O. Abe, Y. Nippashi, and H. Yamasue, "Comparison of white matter integrity between autism spectrum disorder subjects and typically developing individuals: a meta-analysis of diffusion tensor imaging tractography studies," Molecular autism, vol. 4, no. 1, p. 25, 2013.

[18] M. Mostapha et al., "Towards non-invasive image-based early diagnosis of autism," in International Conference on Medical Image Computing and Computer-Assisted Intervention. Springer, 2015, pp. 160–168.

[19] R. A. Vasa, S. H. Mostofsky, and J. B. Ewen, "The disrupted connectivity hypothesis of autism spectrum disorders: time for the next phase in research," Biological Psychiatry: Cognitive Neuroscience and Neuroimaging, vol. 1, no. 3, pp. 245–252, 2016.

[20] M. Kuno, Y. Hirano, A. Nakagawa, K. Asano, F. Oshima, S. Nagaoka, K. Matsumoto, Y. Masuda, M. Iyo, and E. Shimizu, "White matter features associated with autistic traits in obsessive-compulsive disorder," Frontiers in psychiatry, vol. 9, p. 216, 2018.

[21] M. Ingalhalikar, D. Parker, L. Bloy, T. P. Roberts, and R. Verma, "Diffusion based abnormality markers of pathology: toward learned diagnostic prediction of asd," Neuroimage, vol. 57, no. 3, pp. 918–927, 2011.

[22] N. Adluru, C. Hinrichs, M. K. Chung, J.-E. Lee, V. Singh, E. D. Bigler, N. Lange, J. E. Lainhart, and A. L. Alexander, "Classification in dti using shapes of white matter tracts," in 2009 Annual International Conference of the IEEE Engineering in Medicine and Biology Society. IEEE, 2009, pp. 2719–2722.

[23] N. Yahata, J. Morimoto, R. Hashimoto, G. Lisi, K. Shibata, Y. Kawakubo, H. Kuwabara, M. Kuroda, T. Yamada, F. Megumi et al., "A small number of abnormal brain connections predicts adult autism spectrum disorder," Nature communications, vol. 7, p. 11254, 2016.

[24] A. L. Alexander et al., "Diffusion tensor imaging of the brain," Neurotherapeutics, vol. 4, no. 3, pp. 316–329, 2007.

[25] A. Kunimatsu et al., "The optimal trackability threshold of fractional anisotropy for diffusion tensor tractography of the corticospinal tract," Magnetic Resonance in Medical Sciences, vol. 3, no. 1, pp. 11–17, 2004.

[26] N. Bodammer et al., "Eddy current correction in diffusion-weighted imaging using pairs of images acquired with opposite diffusion gradient polarity," Magnetic Resonance in Medicine, vol. 51, no. 1, pp. 188–193, 2004.

[27] S. M. Smith, "Fast robust automated brain extraction," Human Brain Mapping, vol. 17, no. 3, pp. 143–155, 2002.

[28] A. Alansary et al., "Infant brain extraction in T1-weighted MR images using BET and refinement using LCDG and MGRF models," IEEE Journal of Biomedical and Health Informatics, vol. 20, no. 3, pp. 925–935, 2016.

[29] S. Mori et al., MRI atlas of human white matter. Amsterdam: Elsevier, 2005.

[30] Y. Wang, A. Gupta, Z. Liu, H. Zhang, M. L. Escolar, J. H. Gilmore, S. Gouttard, P. Fillard, E. Maltbie, G. Gerig et al., "Dti registration in atlas based fiber analysis of infantile krabbe disease," Neuroimage, vol. 55, no. 4, pp. 1577–1586, 2011.

[31] I. Guyon, S. Gunn, M. Nikravesh, and L. A. Zadeh, Feature extraction: foundations and applications. Springer, 2008, vol. 207.

[32] K. Pelphrey. (2014) Multimodal developmental neurogenetics of females with asd. [Online]. Available: https://ndar.nih.gov/edit_collection.html?id=2021

[33] S. S. Panesar, F.-C. Yeh, C. P. Deibert, D. Fernandes-Cabral, V. Rowthu, P. Celtikci, E. Celtikci, W. D. Hula, S. Pathak, and J. C. Fernández-Miranda, "A diffusion spectrum imaging-based tractographic study into the anatomical subdivision and cortical connectivity of the ventral external capsule: uncinate and inferior fronto-occipital fascicles," Neuroradiology, vol. 59, pp. 971–987, 2017.

[34] S. E. Urger, M. D. De Bellis, S. R. Hooper, D. P. Woolley, S. D. Chen, and J. Provenzale, "The superior longitudinal fasciculus in typically developing children and adolescents: diffusion tensor imaging and neuropsychological correlates," Journal of Child Neurology, vol. 30, no. 1, pp. 9–20, 2015.

[35] Ž. Krsnik, V. Majić, L. Vasung, H. Huang, and I. Kostović, "Growth of thalamocortical fibers to the somatosensory cortex in the human fetal brain," Frontiers in Neuroscience, vol. 11, p. 233, 2017.

[36] J. R. Pryweller, K. B. Schauder, A. W. Anderson, J. L. Heacock, J. H. Foss-Feig, C. R. Newsom, W. A. Loring, and C. J. Cascio, "White matter correlates of sensory processing in autism spectrum disorders," NeuroImage: Clinical, vol. 6, pp. 379–387, 2014.

[37] A. Kushki, E. Drumm, M. P. Mobarak, N. Tanel, A. Dupuis, T. Chau, and E. Anagnosou, "Investigating the autonomic nervous system response to anxiety in children with autism spectrum disorders," PLoS One, vol. 8, no. 4, p. e59730, 2013.

[38] A. J. Barkovich and D. Norman, "Anomalies of the corpus callosum: correlation with further anomalies of the brain," AJR, vol. 151, pp. 171–179, 1988.

FIRST A. AUTHOR (M'76–SM'81–F'87) and all authors may include biographies. Biographies are often not included in conference-related papers. This author became a Member (M) of IEEE in 1976, a Senior Member (SM) in 1981, and a Fellow (F) in 1987. The first paragraph may contain a place and/or date of birth (list place, then date). Next, the author's educational background is listed. The degrees should be listed with type of degree in what field, which institution, city, state, and country, and year the degree was earned. The author's major field of study should be lower-cased.

The second paragraph uses the pronoun of the person (he or she) and not the author's last name. It lists military and work experience, including summer and fellowship jobs. Job titles are capitalized. The current job must have a location; previous positions may be listed without one. Information concerning previous publications may be included. Try not to list more than three books or published articles. The format for listing publishers of a book within the biography is: title of book (publisher name, year) similar to a reference. Current and previous research interests end the paragraph. The third paragraph begins with the author's title and last name (e.g., Dr. Smith, Prof. Jones, Mr. Kajor, Ms. Hunter). List any memberships in professional societies other than the IEEE. Finally, list any awards and work for IEEE committees and publications. If a photograph is provided, it should be of good quality, and professional-looking. Following are two examples of an author's biography.

SECOND B. AUTHOR was born in Greenwich Village, New York, NY, USA in 1977. He received the B.S. and M.S. degrees in aerospace engineering from the University of Virginia, Charlottesville, in 2001 and the Ph.D. degree in mechanical engineering from Drexel University, Philadelphia, PA, in 2008.

From 2001 to 2004, he was a Research Assistant with the Princeton Plasma Physics Laboratory. Since 2009, he has been an Assistant Professor with the Mechanical Engineering Department, Texas A&M University, College Station. He is the author of three books, more than 150 articles, and more than 70 inventions. His research interests include high-pressure and high-density nonthermal plasma discharge processes and applications, microscale plasma discharges, discharges in liquids, spectroscopic diagnostics, plasma propulsion, and innovation plasma applications. He is an Associate Editor of the journal Earth, Moon, Planets, and holds two patents.

Dr. Author was a recipient of the International Association of Geomagnetism and Aeronomy Young Scientist Award for Excellence in 2008, and the IEEE Electromagnetic Compatibility Society Best Symposium Paper Award in 2011.

THIRD C. AUTHOR, JR. (M'87) received the B.S. degree in mechanical engineering from National Chung Cheng University, Chiayi, Taiwan, in 2004 and the M.S. degree in mechanical engineering from National Tsing Hua University, Hsinchu, Taiwan, in 2006. He is currently pursuing the Ph.D. degree in mechanical engineering at Texas A&M University, College Station, TX, USA.

From 2008 to 2009, he was a Research Assistant with the Institute of Physics, Academia Sinica, Tapei, Taiwan. His research interest includes the development of surface processing and biological/medical treatment techniques using nonthermal atmospheric pressure plasmas, fundamental study of plasma sources, and fabrication of micro- or nanostructured surfaces.

Mr. Author's awards and honors include the Frew Fellowship (Australian Academy of Science), the I. I. Rabi Prize (APS), the European Frequency and Time Forum Award, the Carl Zeiss Research Award, the William F. Meggers Award and the Adolph Lomb Medal (OSA).